

# Path following control of planar snake robots using a cascaded approach

Pål Liljebäck, Idar U. Haugstuen and Kristin Y. Pettersen

**Abstract**—This paper considers path following control of snake robots along straight paths. The proposed controller propels the snake robot forward according to the motion pattern lateral undulation while simultaneously adjusting the heading of the robot according to a line-of-sight guidance law that steers the robot towards and subsequently along the desired path. Under the assumption that the forward velocity of the snake robot is nonzero and positive, we prove that the proposed path following controller  $\mathcal{K}$ -exponentially stabilizes a snake robot to any desired straight path. The paper presents simulation results that illustrate the effectiveness of the path following controller.

## I. INTRODUCTION

Inspired by biological snakes, snake robots carry the potential of meeting the growing need for robotic mobility in challenging environments. Snake robots consist of serially connected modules capable of bending in one or more planes. The many degrees of freedom of snake robots make them difficult to control, but provide traversability in irregular environments that surpasses the mobility of the more conventional wheeled, tracked and legged forms of robotic mobility.

This paper considers planar path following control of snake robots along straight paths. Straight line path following capabilities are important since they enable a snake robot to follow a desired path given by waypoints interconnected by straight lines. Straight line path following is therefore relevant for many future applications of snake robots, such as automated inspection rounds in inaccessible areas of industrial process facilities or mapping of confined spaces by moving along prescribed paths. Note that this paper considers path following, in contrast to trajectory tracking, where the goal is additionally to control the position of the system along the path. During path following, we steer the system towards and along the path, but do not consider the position of the system along the path.

Research on snake locomotion has been conducted for several decades. Gray [1] conducted empirical and analytical studies of snake locomotion already in the 1940s, and Hirose [2] studied biological snakes and developed mathematical relationships characterizing their motion, such as the *serpenoid curve*. The main emphasis in literature so far has mainly been on achieving forward and turning locomotion. The next step will be not only to achieve locomotion, but also to make the snake robot follow a desired path. The research

on this control problem is still limited. The work in [3] considers trajectory tracking of snake robots where a number of the links are assumed to be wheeled (no-slip constraints) so that the underactuation of the system is removed. Path following of a snake robot with active wheels is considered in [4], but no stability analysis of the controller is presented. The authors have previously employed *Poincaré maps* to study the stability properties of snake locomotion along a straight path [5]. The presented analysis is, however, based on numerical calculations and is thus only valid for a given set of controller parameters.

Research on robotic fish and eel-like mechanisms is relevant to research on snake robots since these mechanisms are very similar. The works in [6]–[8] synthesize gaits for translational and rotational motion of various fish-like mechanisms and propose controllers for tracking straight and curved trajectories. However, an analysis that formally proves that the fish-like mechanisms converge to the desired path still remains.

In this paper, we consider the problem of planar path following control of snake robots. The contribution is a path following controller that enables snake robots to track a planar straight path. Using cascaded systems theory, we show that under the assumption that the forward velocity of the snake robot is nonzero and positive, the proposed controller guarantees  $\mathcal{K}$ -exponential stability of the distance between the snake robot and the desired path and also  $\mathcal{K}$ -exponential stability of the heading of the robot with respect to the direction of the path. The paper presents simulation results that illustrate the effectiveness of the proposed controller.

The paper is organized as follows. Section II presents some mathematical preliminaries. Section III presents the model of the snake robot. Section IV presents the path following controller. Section V presents simulation results. Finally, Section VI presents concluding remarks.

## II. MATHEMATICAL PRELIMINARIES

This section presents some stability concepts that are employed in Section IV to analyse the path following controller of the snake robot. Consider the system

$$\dot{\mathbf{x}} = \mathbf{f}(t, \mathbf{x}) \quad (1)$$

where  $f : \mathbb{R}_{\geq 0} \times \mathbb{R}^n \rightarrow \mathbb{R}^n$  is piecewise continuous in  $t$  and locally Lipschitz in  $\mathbf{x}$ .

*Definition 1:* (GUAS, see Lemma 4.5 in [9]). The equilibrium point  $\mathbf{x} = \mathbf{0}$  of the system (1) is *globally uniformly asymptotically stable* (GUAS) if there exists a class  $\mathcal{KL}$  function  $\beta$  such that for any initial state  $\mathbf{x}(t_0)$

$$\|\mathbf{x}(t)\| \leq \beta(\|\mathbf{x}(t_0)\|, t - t_0), \quad \forall t \geq t_0 \geq 0. \quad (2)$$

Affiliation of Pål Liljebäck is shared between the Department of Engineering Cybernetics at the Norwegian University of Science and Technology, NO-7491 Trondheim, Norway, and SINTEF ICT, Dept. of Applied Cybernetics, N-7465 Trondheim, Norway. E-mail: Pal.Liljeback@sintef.no

Idar U. Haugstuen and K. Y. Pettersen are with the Department of Engineering Cybernetics at the Norwegian University of Science and Technology, NO-7491 Trondheim, Norway. E-mail: haugstue@stud.ntnu.no, Kristin.Y.Pettersen@itk.ntnu.no

*Definition 2:* (Global  $\mathcal{K}$ -exponential stability, see Definition 2 in [10]).

The equilibrium point  $\mathbf{x} = \mathbf{0}$  of the system (1) is globally  $\mathcal{K}$ -exponentially stable if there exist a positive constant  $\lambda$  and a class  $\mathcal{K}$  function  $\alpha$  such that for any initial state  $\mathbf{x}(t_0)$

$$\|\mathbf{x}(t)\| \leq \alpha(\|\mathbf{x}(t_0)\|)e^{-\lambda(t-t_0)}, \quad \forall t \geq t_0 \geq 0. \quad (3)$$

A definition of class  $\mathcal{K}$  functions and class  $\mathcal{KL}$  functions is given in [9] (Definition 4.2 and 4.3). Next, consider the cascaded system

$$\dot{\mathbf{x}} = \mathbf{f}_1(t, \mathbf{x}) + \mathbf{g}(t, \mathbf{x}, \mathbf{y})\mathbf{y} \quad (4)$$

$$\dot{\mathbf{y}} = \mathbf{f}_2(t, \mathbf{y}) \quad (5)$$

where  $\mathbf{x} \in \mathbb{R}^n$ ,  $\mathbf{y} \in \mathbb{R}^m$ ,  $\mathbf{f}_1(t, \mathbf{x})$  is continuously differentiable in  $(t, \mathbf{x})$ , and  $\mathbf{f}_2(t, \mathbf{y})$ ,  $\mathbf{g}(t, \mathbf{x}, \mathbf{y})$  are continuous in their arguments and locally Lipschitz in  $\mathbf{y}$  and  $(\mathbf{x}, \mathbf{y})$ , respectively.

*Theorem 3:* (See Theorem 2 in [11]).

The cascaded system (4), (5) is GUAS if the following three assumptions are satisfied:

**(A1)** The system  $\dot{\mathbf{x}} = \mathbf{f}_1(t, \mathbf{x})$  is GUAS with a radially unbounded Lyapunov function satisfying

$$\left\| \frac{\partial V}{\partial \mathbf{x}} \right\| \|\mathbf{x}\| \leq cV(t, \mathbf{x}), \quad \forall \|\mathbf{x}\| \geq \eta \quad (6)$$

where  $c > 0$  and  $\eta > 0$  are constants.

**(A2)** The function  $\mathbf{g}(t, \mathbf{x}, \mathbf{y})$  satisfies

$$\|\mathbf{g}(t, \mathbf{x}, \mathbf{y})\| \leq \theta_1(\|\mathbf{y}\|) + \theta_2(\|\mathbf{y}\|)\|\mathbf{x}\| \quad (7)$$

where  $\theta_1, \theta_2 : \mathbb{R}_{\geq 0} \rightarrow \mathbb{R}_{\geq 0}$  are continuous.

**(A3)** The system  $\dot{\mathbf{y}} = \mathbf{f}_2(t, \mathbf{y})$  is GUAS and for all  $t_0 \geq 0$

$$\int_{t_0}^{\infty} \|\mathbf{y}(t)\| dt \leq \kappa(\|\mathbf{y}(t_0)\|) \quad (8)$$

where the function  $\kappa(\cdot)$  is a class  $\mathcal{K}$  function.

*Lemma 4:* (See Lemma 8 in [12]).

If in addition to the assumptions in Theorem 3 both  $\dot{\mathbf{x}} = \mathbf{f}_1(t, \mathbf{x})$  and  $\dot{\mathbf{y}} = \mathbf{f}_2(t, \mathbf{y})$  are globally  $\mathcal{K}$ -exponentially stable, then the cascaded system (4), (5) is globally  $\mathcal{K}$ -exponentially stable.

### III. THE MODEL OF THE SNAKE ROBOT

This section summarizes the model of the snake robot which the controller development in Section IV is based upon. For a more detailed presentation of the model, the reader is referred to [13].

#### A. Overview of the model

We consider a planar snake robot with links interconnected by active revolute joints. The surface beneath the robot is flat and horizontal, and each link is subjected to a viscous ground friction force. The body shape changes of the robot induce friction forces on the links that produce the translational and rotational motion of the robot. A simplified model that captures only the most essential part of the snake robot dynamics is proposed in [13]. The idea behind this model is illustrated in Fig. 1 and motivated by an analysis presented in [13], which shows that:

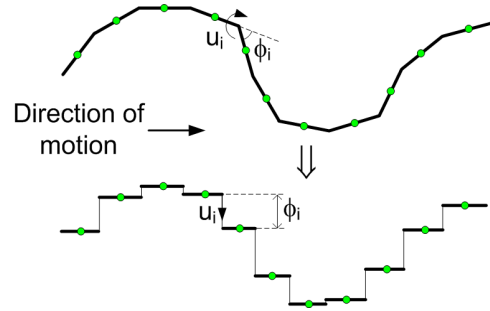


Fig. 1. The revolute joints of the snake robot are modelled as prismatic joints that displace the CM of each link transversal to the direction of motion.

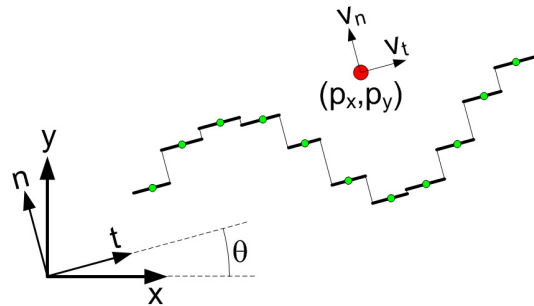


Fig. 2. Illustration of the two coordinate frames employed in the model. The global  $x$ - $y$  frame is fixed. The  $t$ - $n$  frame is always aligned with the snake robot.

- The forward motion of a planar snake robot is produced by the link velocity components that are *normal* to the forward direction.
- The change in body shape during forward locomotion primarily consists of relative displacements of the CM of the links *normal* to the forward direction of motion.

Based on these two properties, the simplified model describes the body shape changes of a snake robot as *linear displacements* of the links with respect to each other instead of rotational displacements. The linear displacements occur *normal* to the forward direction of motion and produce friction forces that propel the robot forward. This essentially means that the revolute joints of the snake robot are modelled as prismatic (translational) joints and that the rotational motion of the links during body shape changes is disregarded. However, the model still captures the *effect* of the rotational link motion during body shape changes, which is a linear displacement of the CM of the links normal to the forward direction of motion.

The mathematical model of the snake robot is summarized in the next subsection in terms of the symbols illustrated in Fig. 2 and Fig. 3.

#### B. Equations of motion

The snake robot has  $N$  links of length  $l$  and mass  $m$  interconnected by  $N-1$  prismatic joints. The prismatic joints control the normal direction distance between the links. As seen in Fig. 3, the normal direction distance from link  $i$  to

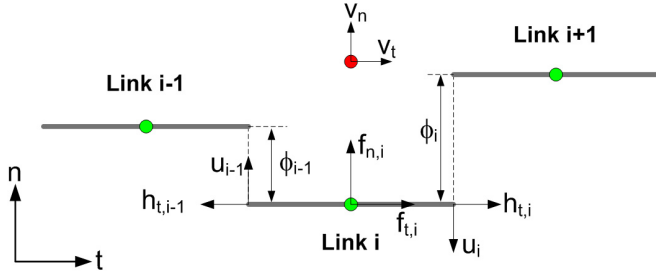


Fig. 3. Symbols characterizing the kinematics and dynamics of the snake robot.

link  $i + 1$  is denoted by  $\phi_i$  and represents the coordinate of joint  $i$ . The positive direction of  $\phi_i$  is along the  $n$  axis.

The snake robot moves in the horizontal plane and has  $N + 2$  degrees of freedom. The motion is defined with respect to the two coordinate frames illustrated in Fig. 2. The  $x$ - $y$  frame is the fixed global frame. The  $t$ - $n$  frame is always aligned with the snake robot, i.e. the  $t$  and  $n$  axis always point in the *tangential* and *normal* direction of the robot, respectively. The origin of both frames are fixed and coincide.

As seen in Fig. 2, the global frame position of the CM (center of mass) of the snake robot is denoted by  $(p_x, p_y) \in \mathbb{R}^2$ . The global frame orientation, denoted by  $\theta \in \mathbb{R}$ , is defined as the angle between the  $t$  axis and the global  $x$  axis with counterclockwise positive direction.

The state vector of the system is chosen as

$$\mathbf{x} = (\phi, \theta, p_x, p_y, \mathbf{v}_\phi, v_\theta, v_t, v_n) \in \mathbb{R}^{2N+4} \quad (9)$$

where  $\phi = (\phi_1, \dots, \phi_{N-1}) \in \mathbb{R}^{N-1}$  are the joint coordinates,  $\theta \in \mathbb{R}$  is the absolute orientation,  $(p_x, p_y) \in \mathbb{R}^2$  is the global frame position of the CM,  $\mathbf{v}_\phi = \dot{\phi} \in \mathbb{R}^{N-1}$  are the joint velocities,  $v_\theta = \dot{\theta} \in \mathbb{R}$  is the angular velocity, and  $(v_t, v_n) \in \mathbb{R}^2$  is the tangential and normal direction velocity of the snake robot. Note that we define the position with respect to the global frame, but the translational velocity with respect to the  $t$ - $n$  frame.

As illustrated in Fig. 3, each link is influenced by a ground friction force (acting on the CM of the link) and constraint forces that hold the joints together. A model of these forces is presented in [13], where it is also shown that the complete model of the snake robot can be written as

$$\dot{\phi} = \mathbf{v}_\phi \quad (10a)$$

$$\dot{\theta} = v_\theta \quad (10b)$$

$$\dot{p}_x = v_t \cos \theta - v_n \sin \theta \quad (10c)$$

$$\dot{p}_y = v_t \sin \theta + v_n \cos \theta \quad (10d)$$

$$\dot{\mathbf{v}}_\phi = -\frac{c_1}{m} \mathbf{v}_\phi + \frac{c_2}{m} v_t \mathbf{A} \mathbf{D}^T \phi + \frac{1}{m} \mathbf{D} \mathbf{D}^T \mathbf{u} \quad (10e)$$

$$\dot{v}_\theta = -c_3 v_\theta + \frac{c_4}{N-1} v_t \bar{\mathbf{e}}^T \phi \quad (10f)$$

$$\dot{v}_t = -\frac{c_1}{m} v_t + \frac{2c_2}{Nm} v_n \bar{\mathbf{e}}^T \phi - \frac{c_2}{Nm} \phi^T \mathbf{A} \bar{\mathbf{D}} \mathbf{v}_\phi \quad (10g)$$

$$\dot{v}_n = -\frac{c_1}{m} v_n + \frac{2c_2}{Nm} v_t \bar{\mathbf{e}}^T \phi \quad (10h)$$

where  $\mathbf{u} \in \mathbb{R}^{N-1}$  are the actuator forces at the joints and  $\bar{\mathbf{e}} = [1 \ \dots \ 1]^T \in \mathbb{R}^{N-1}$ ,

$$\bar{\mathbf{D}} = \mathbf{D}^T (\mathbf{D} \mathbf{D}^T)^{-1} \in \mathbb{R}^{N \times (N-1)},$$

$$\mathbf{A} = \begin{bmatrix} 1 & 1 & & & \\ & & \ddots & & \\ & & & 1 & 1 \\ & & & & & \ddots & & \\ & & & & & & 1 & 1 \end{bmatrix}, \mathbf{D} = \begin{bmatrix} 1 & -1 & & & \\ & & \ddots & & \\ & & & & & \ddots & & \\ & & & & & & 1 & -1 \end{bmatrix},$$

where  $\mathbf{A} \in \mathbb{R}^{(N-1) \times N}$  and  $\mathbf{D} \in \mathbb{R}^{(N-1) \times N}$ . The parameters  $c_1$ ,  $c_2$ ,  $c_3$ , and  $c_4$  are scalar friction coefficients that characterize the external forces acting on the snake robot. In particular, the coefficient  $c_1$  determines the magnitude of the friction forces resisting the link motion,  $c_2$  determines the magnitude of the induced friction forces that propel the snake robot forward,  $c_3$  determines the friction torque opposing the rotation of the snake robot, while  $c_4$  determines the induced torque that rotates the snake robot. This torque is induced when the forward direction velocity and the average of the joint coordinates are nonzero. The role of each coefficient is explained in more detail in [13].

#### IV. DESIGN AND ANALYSIS OF THE PATH FOLLOWING CONTROLLER

In this section, we design and analyse a straight line path following controller for the snake robot.

##### A. Control objective

The control objective is to steer the snake robot so that it converges to and subsequently tracks a straight path while maintaining a heading which is parallel to the path. To this end, we define the global coordinate system so that the global  $x$  axis is aligned with the desired straight path. The position of the snake robot along the global  $y$  axis,  $p_y$ , is thereby the shortest distance from the robot to the desired path and the orientation of the snake robot,  $\theta$ , is the angle that the robot forms with the desired path. The control objective is thereby to regulate  $p_y$  and  $\theta$  to zero. Since snake robot locomotion is a slow form of robotic mobility which is generally employed for traversability purposes, the authors consider it less important to accurately control the forward velocity of the robot. During path following with a snake robot, it therefore makes sense to focus all the control efforts on converging to the path and subsequently progressing along the path at some nonzero forward velocity  $v_t \in [V_{\min}, V_{\max}]$ , where  $V_{\min}$  and  $V_{\max}$  represent the boundaries of some positive interval in which we would like the forward velocity to be contained.

From the above discussion, the control problem is to design a (possibly time-varying) feedback control law

$$\mathbf{u} = \mathbf{u}(t, \phi, \theta, p_y, \mathbf{v}_\phi, v_\theta, v_t, v_n) \in \mathbb{R}^{N-1} \quad (11)$$

such that the following control objectives are reached:

$$\lim_{t \rightarrow \infty} p_y(t) = 0 \quad (12)$$

$$\lim_{t \rightarrow \infty} \theta(t) = 0 \quad (13)$$

## B. Assumptions

A planar snake robot achieves forward motion through periodic body shape changes that generate external forces on the robot from the environment, which propel the robot forward. The most common form of such periodic body shape changes is called *lateral undulation* [2] and consists of horizontal waves that are propagated backwards along the snake body from head to tail. The work by the authors in [14], which investigates the velocity dynamics of a snake robot during lateral undulation, shows that the forward velocity during lateral undulation oscillates around a positive nonzero average velocity that can be predetermined based on the parameters characterizing the gait pattern. In other words, when the snake robot conducts lateral undulation, the results in [14] suggest that the forward velocity is contained in some nonzero and positive interval  $[V_{\min}, V_{\max}]$  that can be scaled based on a set of gait pattern parameters. We therefore choose to base the path following controller of the snake robot on the following assumption:

*Assumption 5:* The snake robot conducts *lateral undulation* and has a forward velocity which is always nonzero and positive, i.e.  $v_t \in [V_{\min}, V_{\max}] \forall t \geq 0$  where  $V_{\max} \geq V_{\min} > 0$ .

## C. Model transformation

On the basis of Assumption 5, we will disregard the dynamics of the forward velocity  $v_t$  given by (10g) and instead treat the forward velocity as a positive parameter satisfying  $v_t \in [V_{\min}, V_{\max}]$ .

As seen in (10f) and (10h), the joint coordinates  $\phi$  are present in the dynamics of both the angular velocity  $v_\theta$  and the sideways velocity  $v_n$  of the snake robot. This complicates the controller design since the body shape changes will affect both the heading and the sideways motion of the robot. Motivated by [15], we see that it is possible to remove the effect of  $\phi$  on the sideways velocity by the coordinate transformation:

$$\bar{p}_x = p_x + \epsilon \cos \theta \quad (14a)$$

$$\bar{p}_y = p_y + \epsilon \sin \theta \quad (14b)$$

$$\bar{v}_n = v_n + \epsilon v_\theta \quad (14c)$$

where  $\epsilon$  is a constant parameter defined as

$$\epsilon = -\frac{2(N-1)c_2}{Nm} \frac{c_2}{c_4} \quad (15)$$

With the new coordinates in (14), the model (10) is transformed into

$$\dot{\bar{\phi}} = \mathbf{v}_\phi \quad (16a)$$

$$\dot{\bar{\theta}} = v_\theta \quad (16b)$$

$$\dot{\bar{p}}_x = v_t \cos \theta - \bar{v}_n \sin \theta \quad (16c)$$

$$\dot{\bar{p}}_y = v_t \sin \theta + \bar{v}_n \cos \theta \quad (16d)$$

$$\dot{\mathbf{v}}_\phi = -\frac{c_1}{m} \mathbf{v}_\phi + \frac{c_2}{m} v_t \mathbf{A} \mathbf{D}^T \phi + \frac{1}{m} \mathbf{D} \mathbf{D}^T \mathbf{u} \quad (16e)$$

$$\dot{v}_\theta = -c_3 v_\theta + \frac{c_4}{N-1} v_t \bar{\mathbf{e}}^T \phi \quad (16f)$$

$$\dot{\bar{v}}_n = X v_\theta + Y \bar{v}_n \quad (16g)$$

where, by Assumption 5, the parameter  $v_t \in [V_{\min}, V_{\max}]$  and  $V_{\max} \geq V_{\min} > 0$ , and where

$$X = \epsilon \left( \frac{c_1}{m} - c_3 \right) \quad (17a)$$

$$Y = -\frac{c_1}{m} \quad (17b)$$

The two scalar constants  $X$  and  $Y$  have been introduced in (16g) for simplicity of notation in the following sections.

*Remark 6:* The coordinate transformation (14) is illustrated to the left in Fig. 4 and can be interpreted as moving the point that determines the position of the snake robot a distance  $\epsilon$  along the tangential direction of the robot to a new location, which is precisely where the body shape changes of the robot (characterized by  $\bar{\mathbf{e}}^T \phi$ ) generate a pure rotational motion and no sideways force.

## D. The path following controller

The path following controller of the snake robot consists of two main components. The first component is the gait pattern controller, which propels the snake robot forward according to the gait pattern *lateral undulation* (as stated in Assumption 5). The second component is the heading controller, which steers the snake robot towards and subsequently along the desired path. The two components of the path following controller are now presented.

1) *Gait pattern controller:* As proposed in [2], lateral undulation is achieved by controlling joint  $i \in \{1, \dots, N-1\}$  of the snake robot according to the sinusoidal reference

$$\phi_{i,\text{ref}} = \alpha \sin(\omega t + (i-1)\delta) + \phi_o \quad (18)$$

where  $\alpha$  and  $\omega$  are the amplitude and frequency, respectively, of the sinusoidal joint motion and  $\delta$  determines the phase shift between the joints. The parameter  $\phi_o$  is a joint offset coordinate that the heading controller will use to control the direction of the locomotion. As shown in [16], the average forward velocity  $\bar{v}_t$  of the snake robot during straight path motion is given by

$$\bar{v}_t = \frac{c_2}{2Nc_1} \alpha^2 \omega k_\delta \quad (19)$$

where  $k_\delta$  is a constant parameter determined by the phase shift  $\delta$ . This relation can be used to choose the gait parameters  $\alpha$ ,  $\omega$ , and  $\delta$  in order to achieve the desired average forward velocity.

In order to make the joints track the joint reference coordinates given by (18), we set the actuator forces according to the linearizing control law

$$\mathbf{u} = m \left( \mathbf{D} \mathbf{D}^T \right)^{-1} \left( \bar{\mathbf{u}} + \frac{c_1}{m} \dot{\bar{\phi}} - \frac{c_2}{m} v_t \mathbf{A} \mathbf{D}^T \phi \right) \quad (20)$$

where  $\bar{\mathbf{u}} \in \mathbb{R}^{N-1}$  is a new set of control inputs. This control law transforms the joint dynamics (16e) into  $\dot{\mathbf{v}}_\phi = \ddot{\bar{\phi}} = \bar{\mathbf{u}}$ . Subsequently, we choose the new control input  $\bar{\mathbf{u}}$  as

$$\bar{\mathbf{u}} = \ddot{\phi}_{\text{ref}} + k_{v_\phi} \left( \dot{\phi}_{\text{ref}} - \dot{\bar{\phi}} \right) + k_\phi \left( \phi_{\text{ref}} - \phi \right) \quad (21)$$

where  $k_\phi > 0$  and  $k_{v_\phi} > 0$  are scalar controller gains and  $\phi_{\text{ref}} = (\phi_{1,\text{ref}}, \dots, \phi_{N-1,\text{ref}}) \in \mathbb{R}^{N-1}$  are the joint reference coordinates given by (18). By introducing the error variable

$$\tilde{\phi} = \phi - \phi_{\text{ref}} \quad (22)$$

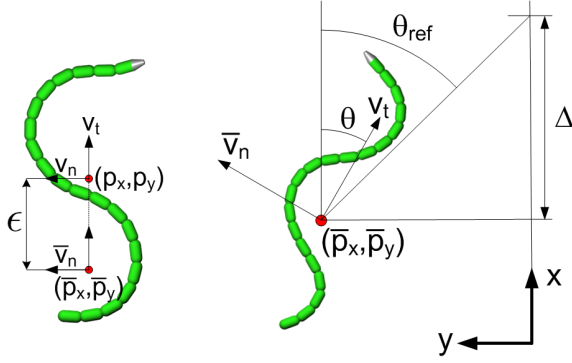


Fig. 4. Left: The coordinate transformation of the snake robot. Right: The Line-of-Sight (LOS) guidance system.

the resulting error dynamics of the joints can be written as

$$\ddot{\tilde{\phi}} + k_{v_\phi} \dot{\tilde{\phi}} + k_\phi \tilde{\phi} = 0 \quad (23)$$

which is clearly *exponentially stable* [9]. This means that the joint coordinates exponentially track the reference coordinates given by (18).

2) *Heading controller*: In order to steer the snake robot towards the desired straight path, we employ the Line-of-Sight (LOS) guidance law

$$\theta_{\text{ref}} = -\arctan\left(\frac{\bar{p}_y}{\Delta}\right) \quad (24)$$

where  $\bar{p}_y$  is the cross-track error and  $\Delta > 0$  is a design parameter referred to as the *look-ahead distance*. This LOS guidance law is commonly used during e.g. path following control of marine surface vessels [15], [17]. As illustrated to the right in Fig. 4, the LOS angle  $\theta_{\text{ref}}$  corresponds to the orientation of the snake robot when it is headed towards the point located a distance  $\Delta$  ahead of the snake robot along the desired path. The value of  $\Delta$  is important since it will determine the rate of convergence to the desired path.

As mentioned in Section IV-D.1, we will use the joint offset coordinate  $\phi_o$  in (18) to ensure that the heading of the snake robot  $\theta$  tracks the LOS angle given by (24). Motivated by [15] and [18], we conjecture that making  $\theta$  track the LOS angle  $\theta_{\text{ref}}$  will make the snake converge to the desired path and subsequently follow the path with its heading parallel to the path. In other words, we conjecture that a control law making  $\theta$  track  $\theta_{\text{ref}}$  will fulfill the control objectives (12) and (13). To derive the control law for  $\phi_o$ , we first rewrite the dynamics of  $v_\theta$  given by (16f) as a function of the joint reference coordinates given by (18). From (22), we have that  $\phi = \phi_{\text{ref}} + \tilde{\phi}$ . Using (18), we can therefore rewrite (16f) as

$$\begin{aligned} \dot{v}_\theta &= -c_3 v_\theta + c_4 v_t \phi_o \\ &+ \frac{c_4}{N-1} v_t \left( \sum_{i=1}^{N-1} \alpha \sin(\omega t + (i-1)\delta) + \bar{e}^T \tilde{\phi} \right) \end{aligned} \quad (25)$$

Consequently, choosing  $\phi_o$  as

$$\begin{aligned} \phi_o &= \frac{1}{c_4 v_t} \left( \ddot{\theta}_{\text{ref}} + c_3 \dot{\theta}_{\text{ref}} - k_\theta (\theta - \theta_{\text{ref}}) \right. \\ &\quad \left. - \frac{c_4}{N-1} v_t \sum_{i=1}^{N-1} \alpha \sin(\omega t + (i-1)\delta) \right) \end{aligned} \quad (26)$$

where  $k_\theta > 0$  is a scalar controller gain, enables us to write the error dynamics of the heading angle  $\theta$  as

$$\ddot{\tilde{\theta}} + c_3 \dot{\tilde{\theta}} + k_\theta \tilde{\theta} = \frac{c_4}{N-1} v_t \bar{e}^T \tilde{\phi} \quad (27)$$

where we have introduced the error variable

$$\tilde{\theta} = \theta - \theta_{\text{ref}} \quad (28)$$

*Remark 7*: The joint coordinate offset in (26) depends on the inverse of the forward velocity  $v_t$ . This does not represent a problem since, by Assumption 5, the forward velocity is always nonzero. The implementation of the path following controller must ensure that the controller is activated *after* the snake robot has obtained a positive forward velocity.

*Remark 8*: The error dynamics of the joints in (23) and the error dynamics of the heading in (27) represent a cascaded system. In particular, the system (23) perturbs the system (27) through the interconnection term  $\frac{c_4}{N-1} v_t \bar{e}^T \tilde{\phi}$ . Using cascaded systems theory, it will be shown in Section IV-F that the origin of this cascaded system is globally  $\mathcal{K}$ -exponentially stable.

We have now presented the complete path following controller of the snake robot. The structure of the complete controller is summarized in Fig. 5.

#### E. Main result

Based on the guidance and control laws presented in the previous subsection, we now formulate the main result of this paper.

*Theorem 9*: Consider a planar snake robot described by the model (16) and suppose that Assumption 5 is satisfied. If the parameter  $\Delta$  of the LOS guidance law (24) is chosen such that

$$\Delta > \frac{|X|}{|Y|} \left( 1 + \frac{V_{\text{max}}}{V_{\text{min}}} \right) \quad (29)$$

then the path following controller defined by (18), (20), (21), (24), and (26) guarantees that the control objectives (12) and (13) are achieved for any set of initial conditions satisfying  $v_t \in [V_{\text{min}}, V_{\text{max}}]$ .

*Proof*: The proof of this theorem is given in Section IV-F.  $\blacksquare$

*Remark 10*: Theorem 9 does not specify the boundary values  $V_{\text{min}}$  and  $V_{\text{max}}$  of the interval in which the forward velocity  $v_t$  is contained. By Assumption 5, however, there exists a positive interval that contains  $v_t$  for all time  $t \geq 0$ . In practice, conservative values for these boundary values can be chosen, but in order to achieve a tighter bound on  $\Delta$ , we would like to specify  $V_{\text{min}}$  and  $V_{\text{max}}$  as a function of the gait pattern parameters  $\alpha$ ,  $\omega$ ,  $\delta$ , and  $\phi_o$ . This remains a topic of future work.

#### F. Proof of the main result

We will prove Theorem 9 in three steps. In the first step, we show that the complete system, including the path following controller, can be written as a cascaded system. In the second step, we prove stability of the nominal systems in the cascade. Finally, we derive bounds on the interconnection terms between the nominal systems, which, by Theorem 3 and Lemma 4, allow us to conclude stability of the complete

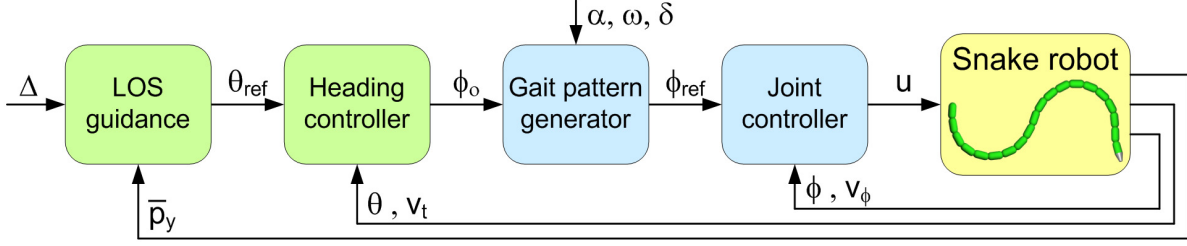


Fig. 5. The structure of the path following controller.

cascaded system. We will follow the steps of a similar proof presented in [19].

We begin by rewriting the dynamics of the cross-track error  $\bar{p}_y$  and the sideways velocity  $\bar{v}_n$  in terms of the heading error  $\theta$ . From (28) and (24) we have that

$$\theta = -\arctan\left(\frac{\bar{p}_y}{\Delta}\right) + \tilde{\theta} \quad (30)$$

By using the relations  $\sin(-\arctan(\frac{\bar{p}_y}{\Delta})) = -\frac{\bar{p}_y}{\sqrt{\bar{p}_y^2 + \Delta^2}}$  and  $\cos(-\arctan(\frac{\bar{p}_y}{\Delta})) = \frac{\Delta}{\sqrt{\bar{p}_y^2 + \Delta^2}}$ , it can be verified that (16d) can be rewritten as

$$\dot{\bar{p}}_y = -\frac{v_t}{\sigma}\bar{p}_y + \frac{\Delta}{\sigma}\bar{v}_n + \gamma\tilde{\theta} \quad (31)$$

where

$$\sigma = \sqrt{\bar{p}_y^2 + \Delta^2} \quad (32)$$

$$\gamma = \frac{\sin\tilde{\theta}}{\tilde{\theta}} \frac{(v_t\Delta + \bar{v}_n\bar{p}_y)}{\sigma} + \frac{1 - \cos\tilde{\theta}}{\tilde{\theta}} \frac{(v_t\bar{p}_y - \bar{v}_n\Delta)}{\sigma} \quad (33)$$

Through similar manipulations, we can rewrite (16g) as

$$\dot{\bar{v}}_n = \frac{X\Delta v_t}{\sigma^3}\bar{p}_y + \left(Y - \frac{X\Delta^2}{\sigma^3}\right)\bar{v}_n - \frac{X\Delta}{\sigma^2}\gamma\tilde{\theta} + X\dot{\tilde{\theta}} \quad (34)$$

Introducing the error variables

$$\boldsymbol{\eta} = \begin{bmatrix} \tilde{\phi} \\ \dot{\tilde{\phi}} \end{bmatrix} \in \mathbb{R}^{2N-2}, \quad \boldsymbol{\xi} = \begin{bmatrix} \tilde{\theta} \\ \dot{\tilde{\theta}} \end{bmatrix} \in \mathbb{R}^2 \quad (35)$$

and using (23), (27), (31), and (34), the model of the snake robot (16) during path following can be written as

$$\begin{bmatrix} \dot{\bar{p}}_y \\ \dot{\bar{v}}_n \end{bmatrix} = \mathbf{C}(\bar{p}_y) \begin{bmatrix} \bar{p}_y \\ \bar{v}_n \end{bmatrix} + \mathbf{H}_\xi(\bar{p}_y, \bar{v}_n, \boldsymbol{\xi})\boldsymbol{\xi} \quad (36a)$$

$$\dot{\boldsymbol{\xi}} = \begin{bmatrix} 0 & 1 \\ -k_\theta & -c_3 \end{bmatrix} \boldsymbol{\xi} + \mathbf{H}_\eta \boldsymbol{\eta} \quad (36b)$$

$$\dot{\boldsymbol{\eta}} = \begin{bmatrix} \mathbf{0} & \mathbf{I} \\ -k_\phi \mathbf{I} & -k_{v_\phi} \mathbf{I} \end{bmatrix} \boldsymbol{\eta} \quad (36c)$$

where  $\mathbf{I} \in \mathbb{R}^{(N-1) \times (N-1)}$  is the identity matrix and

$$\mathbf{H}_\eta = \begin{bmatrix} \mathbf{0} & \mathbf{0} \\ \frac{c_4}{N-1} v_t \bar{\mathbf{e}}^T & \mathbf{0} \end{bmatrix} \quad (37)$$

$$\mathbf{H}_\xi(\bar{p}_y, \bar{v}_n, \boldsymbol{\xi}) = \begin{bmatrix} \gamma & 0 \\ -\frac{X\Delta}{\sigma^2}\gamma & X \end{bmatrix} \quad (38)$$

$$\mathbf{C}(\bar{p}_y) = \begin{bmatrix} -\frac{v_t}{\sigma} & \frac{\Delta}{\sigma} \\ \frac{X\Delta v_t}{\sigma^3} & \left(Y - \frac{X\Delta^2}{\sigma^3}\right) \end{bmatrix} \quad (39)$$

The system (36) is a cascaded system. In particular, the  $\boldsymbol{\eta}$ -dynamics in (36c) perturbs the  $\boldsymbol{\xi}$ -dynamics in (36b) through the interconnection term  $\mathbf{H}_\eta \boldsymbol{\eta}$ , and the  $\boldsymbol{\xi}$ -dynamics perturbs the  $(\bar{p}_y, \bar{v}_n)$ -dynamics in (36a) through the interconnection term  $\mathbf{H}_\xi(\bar{p}_y, \bar{v}_n, \boldsymbol{\xi})\boldsymbol{\xi}$ .

We now investigate the stability of the nominal systems of the cascade, i.e. all parts of (36) except the interconnection terms. The origin  $\boldsymbol{\eta} = \mathbf{0}$  of the linear system (36c) and the origin  $\boldsymbol{\xi} = \mathbf{0}$  of the linear nominal system in (36b) are *globally exponentially stable* since the system matrices clearly are Hurwitz for  $k_\theta, c_3, k_\phi, k_{v_\phi} > 0$  (see Definition 4.5 in [9]). The nominal system of (36a), which is given by

$$\begin{bmatrix} \dot{\bar{p}}_y \\ \dot{\bar{v}}_n \end{bmatrix} = \mathbf{C}(\bar{p}_y) \begin{bmatrix} \bar{p}_y \\ \bar{v}_n \end{bmatrix} \quad (40)$$

is identical to a system considered in [19] in conjunction with path following control of a marine surface vessel. It is shown in [19] that (40) is globally  $\mathcal{K}$ -exponentially stable with a quadratic Lyapunov function as long as the look-ahead distance satisfies

$$\Delta > \frac{|X|}{|Y|} \left(1 + \frac{V_{\max}}{V_{\min}}\right) \quad (41)$$

This corresponds to condition (29) in Theorem 9. Due to space restrictions, we will not repeat this proof here. Since exponential stability implies  $\mathcal{K}$ -exponential stability, we can conclude that all nominal systems of the cascade (36) are globally  $\mathcal{K}$ -exponentially stable.

Next, we derive bounds on the interconnection terms in the cascade. The induced 2-norm of the matrix  $\mathbf{H}_\eta$  satisfies (see Appendix A in [9])

$$\|\mathbf{H}_\eta\|_2 \leq \sqrt{2N-2} \max_j \sum_{i=1}^2 \{\mathbf{H}_\eta\}_{ij} \leq \frac{\sqrt{2}c_4 V_{\max}}{\sqrt{N-1}} \quad (42)$$

while the induced 2-norm of the matrix  $\mathbf{H}_\xi(\bar{p}_y, \bar{v}_n, \boldsymbol{\xi})$  satisfies

$$\begin{aligned} \|\mathbf{H}_\xi\|_2 &\leq \sqrt{2} \max_j \sum_{i=1}^2 \{\mathbf{H}_\xi\}_{ij} \\ &\leq \sqrt{2} \max \left( |\gamma| + \frac{|X|\Delta}{\sigma^2} |\gamma|, |X| \right) \\ &\leq \sqrt{2} \left( |\gamma| + \frac{|X|\Delta}{\sigma^2} |\gamma| + |X| \right) \end{aligned} \quad (43)$$

The function  $\gamma$  given by (33) is bounded according to

$$\begin{aligned} \gamma &\leq \left| \frac{\sin\tilde{\theta}}{\tilde{\theta}} \right| \frac{V_{\max}\Delta + |\bar{v}_n||\bar{p}_y|}{\sigma} + \left| \frac{1 - \cos\tilde{\theta}}{\tilde{\theta}} \right| \frac{V_{\max}|\bar{p}_y| + |\bar{v}_n|\Delta}{\sigma} \\ &\leq \frac{V_{\max}\Delta}{\sigma} + \frac{|\bar{v}_n||\bar{p}_y|}{\sigma} + \frac{V_{\max}|\bar{p}_y|}{\sigma} + \frac{|\bar{v}_n|\Delta}{\sigma} \\ &\leq 2V_{\max} + 2|\bar{v}_n| \end{aligned} \quad (44)$$

By inserting (44) into (43), it is straightforward to verify that

$$\|\mathbf{H}_\xi\|_2 \leq \mathcal{F}_1 + \mathcal{F}_2 \left\| \begin{bmatrix} \bar{p}_y \\ \bar{v}_n \end{bmatrix} \right\|_2 \quad (45)$$

where

$$\mathcal{F}_1 = \sqrt{2} \left( 2V_{\max} \left( 1 + \frac{|X|}{\Delta} \right) + |X| \right) \quad (46)$$

$$\mathcal{F}_2 = 2\sqrt{2} \left( 1 + \frac{|X|}{\Delta} \right) \quad (47)$$

We are now ready to apply Theorem 3 to the cascaded system (36). We first consider the cascade of (36b) and (36c), for which it is straightforward to verify that Assumptions A1 and A3 of Theorem 3 are satisfied since the system (36c) and the nominal system of (36b) are both *globally exponentially stable*. Furthermore, Assumption A2 is trivially satisfied since  $\|\mathbf{H}_\eta\|_2$  is bounded by the constant derived in (42). The cascaded system (36b), (36c) is therefore GUAS and, by Lemma 4, also globally  $\mathcal{K}$ -exponentially stable.

Next, we consider the cascade of (36a) and (36b), for which Assumption A1 and A3 of Theorem 3 are again satisfied since the nominal system of (36a) and the perturbing system (36b) are both globally  $\mathcal{K}$ -exponentially stable. Furthermore, it follows directly from (45) that Assumption A2 is satisfied. The cascaded system (36a), (36b) is therefore GUAS and, by Lemma 4, also globally  $\mathcal{K}$ -exponentially stable.

In summary, the complete cascaded system (36) is globally  $\mathcal{K}$ -exponentially stable. From (30), this implies that  $\theta(t) \rightarrow 0$ , which means that control objective (13) is achieved. It subsequently follows from (14b) that  $p_y(t) \rightarrow 0$ , which means that control objective (12) is achieved. This completes the proof of Theorem 9.

## V. SIMULATION RESULTS

In order to illustrate the effectiveness of the proposed path following controller, the model of the snake robot (10) and the controller were implemented and simulated in *Matlab R2008b* on a laptop running *Windows XP*. The dynamics were calculated using the *ode45* solver in Matlab with a relative and absolute error tolerance of  $10^{-6}$ .

We considered a snake robot with  $N = 10$  links of length  $l = 0.14$  m and mass  $m = 1$  kg. These parameters characterize a physical snake robot recently developed by the authors. Furthermore, we chose the friction coefficients as  $c_1 = 0.45$ ,  $c_2 = 3$ ,  $c_3 = 0.5$  and  $c_4 = 20$ , and the controller gains as  $k_\phi = 20$ ,  $k_{v_\phi} = 5$ , and  $k_\theta = 0.05$ . The gait parameters were chosen as  $\alpha = 0.1$  m,  $\omega = 70^\circ/\text{s}$ , and  $\delta = 40^\circ$ , which by (19) corresponds to the average forward velocity  $\bar{v}_t = \frac{c_2}{2Nc_1} \alpha^2 \omega k_\delta = 0.1$  m/s. By making the conjecture that the forward velocity will always be contained in the interval  $v_t \in [V_{\min}, V_{\max}] = [0.5\bar{v}_t, 2\bar{v}_t] = [0.05 \text{ m/s}, 0.2 \text{ m/s}]$ , the lower bound on the look-ahead distance  $\Delta$  is given by (29) as  $\Delta > 0.15$  m. During the simulations, we chose the look-ahead distance equal to the length of the snake robot, i.e.  $\Delta = 1.4$  m, which is well above the estimated lower limit.

The initial state of the snake robot was set to  $\phi = \mathbf{0}^\circ$ ,  $\theta = 90^\circ$ ,  $p_x = 0$  m,  $p_y = 1$  m,  $v_\phi = \mathbf{0}^\circ/\text{s}$ ,  $v_\theta = 0^\circ/\text{s}$ ,  $v_t = 0.1$  m/s, and  $v_n = 0$  m/s, i.e. the snake robot was initially oriented along the global  $y$  axis and located 1 m away from

the  $x$  axis with an initial forward velocity of 0.1 m/s, i.e. moving away from the desired path.

Note that the calculation of the control input in (21) and (26) requires the derivative of  $\theta_{\text{ref}}$  and  $\phi_o$  with respect to time. During the simulations, we generated these signals by using a 3rd order low-pass filtering reference model (see e.g. Chapter 5 in [17]).

The simulation results are shown in Fig. 6. From Figures 6(a) and 6(b), we see that the position of the snake robot converges nicely to the desired path (i.e. the  $x$  axis). Fig. 6(a) also shows the configuration of the snake robot at  $t = 1$  s,  $t = 30$  s, and  $t = 70$  s. Note that Fig. 6(b) shows the cross-track error in terms of the  $y$  axis coordinate of the CM of the robot, not the transformed  $y$ -axis coordinate given by (14b). The heading of the snake robot, shown in Fig. 6(e), also converges nicely to zero, i.e. to the direction of the desired path. As seen in Fig. 6(c), the forward velocity is always nonzero and positive, as required by Assumption 5, and converges to the velocity  $\bar{v}_t = \frac{c_2}{2Nc_1} \alpha^2 \omega k_\delta = 0.1$  m/s, which was estimated above. Fig. 6(d) shows the joint coordinate of an arbitrarily chosen joint (joint 5) during the path following. The plot shows a very good tracking of the joint reference coordinates. In summary, the simulation results illustrate that the proposed controller successfully steers the snake robot towards and along the desired straight path.

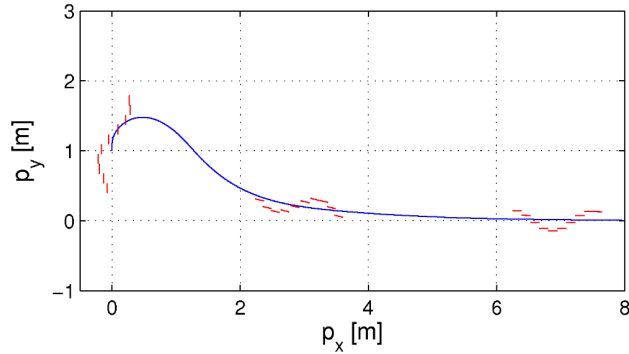
## VI. CONCLUSIONS AND FUTURE WORK

This paper has proposed a path following controller that enables snake robots to track straight paths. Using cascaded systems theory, we have proven that the proposed path following controller  $\mathcal{K}$ -exponentially stabilizes the snake robot to any desired straight path under the assumption that the forward velocity of the robot is nonzero and positive. The paper has presented simulation results that illustrated the effectiveness of the path following controller.

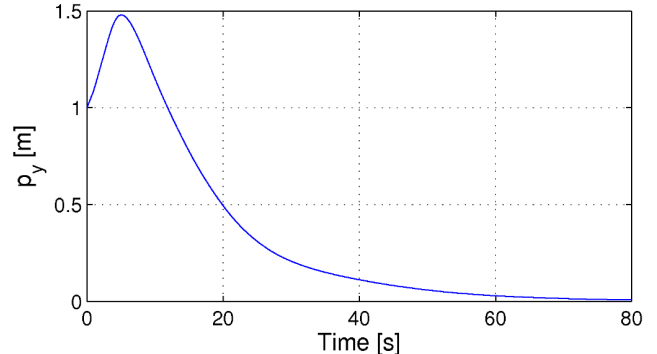
In future work, the authors will specify the bounds on the forward velocity of the snake robot in terms of the gait pattern parameters.

## REFERENCES

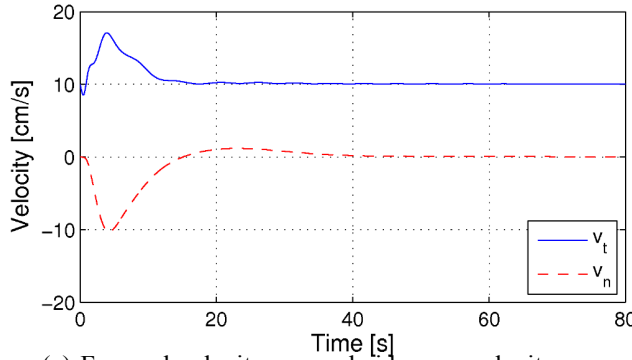
- [1] J. Gray, "The mechanism of locomotion in snakes," *J. Exp. Biol.*, vol. 23, no. 2, pp. 101–120, 1946.
- [2] S. Hirose, *Biologically Inspired Robots: Snake-Like Locomotors and Manipulators*. Oxford: Oxford University Press, 1993.
- [3] F. Matsuno and H. Sato, "Trajectory tracking control of snake robots based on dynamic model," in *Proc. IEEE Int. Conf. on Robotics and Automation*, 2005, pp. 3029–3034.
- [4] B. Murugendran, A. A. Traneth, and S. A. Fjerdingen, "Modeling and path-following for a snake robot with active wheels," in *Proc. IEEE/RSJ Int. Conf. Intelligent Robots and Systems*, 2009, pp. 3643–3650.
- [5] P. Liljebäck, K. Y. Pettersen, Ø. Stavdahl, and J. T. Gravdahl, "Controllability and stability analysis of planar snake robot locomotion," *IEEE Trans. Automatic Control*, 2010, conditionally accepted as Regular Paper.
- [6] P. A. Vela, K. A. Morgansen, and J. W. Burdick, "Underwater locomotion from oscillatory shape deformations," in *Proc. IEEE Conf. Decision and Control*, vol. 2, Dec. 2002, pp. 2074–2080 vol.2.
- [7] K. McIsaac and J. Ostrowski, "Motion planning for anguilliform locomotion," *IEEE Trans. Robot. Autom.*, vol. 19, no. 4, pp. 637–625, August 2003.
- [8] K. Morgansen, B. Triplett, and D. Klein, "Geometric methods for modeling and control of free-swimming fin-actuated underwater vehicles," *IEEE Transactions on Robotics*, vol. 23, no. 6, pp. 1184–1199, Dec 2007.
- [9] H. K. Khalil, *Nonlinear Systems*, 3rd ed. Prentice Hall, 2002.



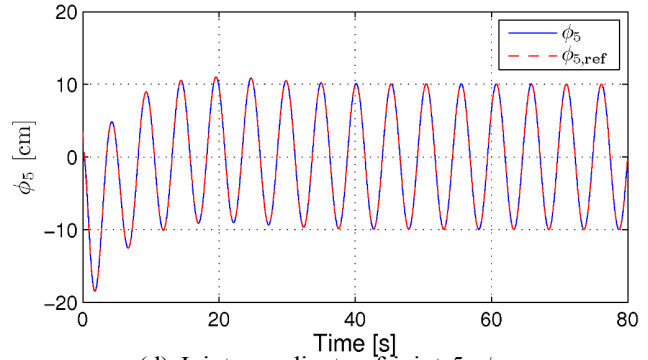
(a) The path of the CM of the snake robot.



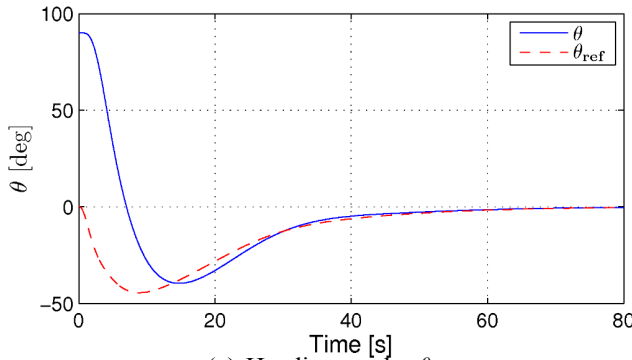
(b) Cross-track error,  $p_y$ .



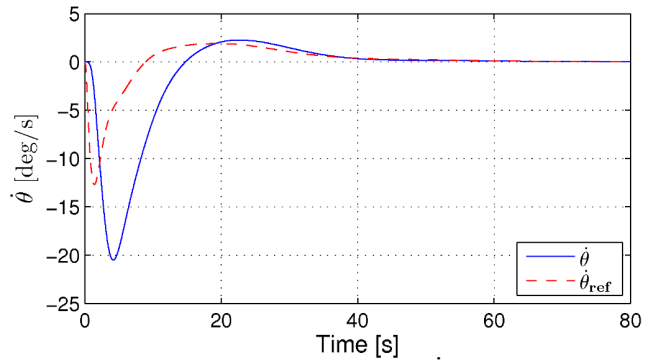
(c) Forward velocity,  $v_t$ , and sideways velocity,  $v_n$ .



(d) Joint coordinate of joint 5,  $\phi_5$ .



(e) Heading angle,  $\theta$ .



(f) Angular velocity,  $\dot{\theta}$ .

Fig. 6. Simulation of straight line path following.

- [10] O. J. Sørдалen and O. Egeland, "Exponential stabilization of non-holonomic chained systems," *IEEE Trans. Automatic Control*, vol. 40, no. 1, pp. 35 – 49, 1995.
- [11] E. Panteley and A. Loria, "On global uniform asymptotic stability of nonlinear time-varying systems in cascade," *Systems & Control Letters*, vol. 33, no. 2, pp. 131 – 138, 1998.
- [12] E. Panteley, E. Lefeber, A. Loria, and H. Nijmeijer, "Exponential tracking control of a mobile car using a cascaded approach," in *Proc. IFAC Workshop on Motion Control*, 1998, pp. 221 – 226.
- [13] P. Liljebäck, K. Y. Pettersen, Ø. Stavdahl, and J. T. Gravdahl, "A simplified model of planar snake robot locomotion," in *Proc. IEEE/RSSJ Int. Conf. Intelligent Robots and Systems*, 2010, accepted.
- [14] —, "Stability analysis of snake robot locomotion based on averaging theory," in *Proc. IEEE Int. Conf. Decision and Control*, 2010, accepted.
- [15] E. Fredriksen and K. Y. Pettersen, "Global  $\kappa$ -exponential way-point maneuvering of ships: Theory and experiments," *Automatica*, vol. 42, pp. 677 – 687, 2006.
- [16] P. Liljebäck, K. Y. Pettersen, Ø. Stavdahl, and J. T. Gravdahl, "Fundamental properties of snake robot locomotion," in *Proc. IEEE/RSSJ Int. Conf. Intelligent Robots and Systems*, 2010, accepted.
- [17] T. I. Fossen, *Marine Control Systems: Guidance, Navigation and Control of Ships, Rigs and Underwater Vehicles*. Trondheim, Norway: Marine Cybernetics, 2002.
- [18] K. Y. Pettersen and E. Lefeber, "Way-point tracking control of ships," in *Proc. IEEE Conf. Decision and Control*, 2001, pp. 940–945.
- [19] A. Pavlov, E. Børhaug, E. Panteley, and K. Y. Pettersen, "Straight line path following for formations of underactuated surface vessels," in *Proc. IFAC NOLCOS*, 2007.